ELSEVIER

Cancer Genetics and Cytogenetics 157 (2005) 109–117

Cancer Genetics and Cytogenetics

Pediatric pancreatoblastoma: histopathologic and cytogenetic characterization of tumor and derived cell line

Linda Barenboim-Stapleton[a], Xuezhong Yang[b], Maria Tsokos[c], Jon M. Wigginton[b], Hesed Padilla-Nash[a], Thomas Ried[a], Carol J. Thiele[b,*]

[a]*Genetics Branch, Center for Cancer Research, National Cancer Institute, National Institutes of Health (NCI/NIH), Bethesda, MD*
[b]*Cell & Molecular Biology Section, Pediatric Oncology Branch, Center for Cancer Research, NCI/NIH, Bethesda, MD 20892*
[c]*Pathology Laboratory, Center for Cancer Research, NCI/NIH, Bethesda, MD*

Received 5 March 2004; received in revised form 21 May 2004; accepted 25 May 2004

Abstract Little is known of the molecular events underlying the genesis of pancreatoblastoma tumors in the pediatric population. Such studies have been limited by the rare nature of the disease, infrequent reports detailing cytogenetic alterations, and the lack of availability of cell lines for biologic studies. We present the isolation of a cell line from a 14-year-old boy with malignant pancreatoblastoma, and its cytogenetic characterization using spectral karyotyping and comparative genomic hybridization (CGH). The cytogenetic analysis revealed an exceedingly complex cytogenetic karyotype, with 33 aberrant chromosomes. CGH revealed multiple regions of chromosomal loss and gain, including a region on 8q gained in adult pancreatic cancers, one that frequently contains the *MYC* oncogene.
© 2005 Elsevier Inc. All rights reserved.

1. Introduction

Pancreatic carcinoma is only the seventh most common tumor in adults, yet it is the fourth most common cause of cancer deaths, after colon, lung, and breast cancer [1]. By contrast, pancreatic tumors are rare in childhood and adolescence and typically have a better outcome if surgically resected [2]. A variety of terms have been used to describe pediatric pancreatic tumors, including acinar, ductal, or islet cell tumors, terms that may reflect differences in the histogenesis of various pancreatic cell types. The two most common pediatric types are pancreatoblastoma (PB) and papillary and solid epithelial neoplasm (PSEN). More than 97% of PSENs are resectable, with only a 3% recurrence. PB is generally considered malignant, because of its capacity for metastasis; however, 75% are resectable and only 13% progress after resection [3].

The molecular events underlying the genesis of PB are unknown, and a cytogenetic picture has been slow to emerge. To date, there are three reported cases of cytogenetic analysis of PB in children [4,5], with chromosome 1 alterations the only common findings. There is an occasional occurrence of PB in association with Beckwith–Wiedemann syndrome, a rare overgrowth syndrome that occurs in ~1 in every 15,000 births (http://cis.nci.nih.gov/fact/3_67.htm). This led Abraham et al. [6] to suggest that, like hepatoblastoma, PB may contain similar genetic alterations. Changes in the APC/β-catenin pathway and chromosome 11p variations were detected in six of nine patients with PB, of whom half were children.

Here we report the case of a 14-year-old boy with a particularly aggressive PB, from which we derived a cell line, CMBS-PB. Traditional banding studies revealed a complex karyotype. We therefore used spectral karyotyping (SKY), which extends traditional cytogenetic techniques and reveals a more detailed analysis of the complex karyotypes that are frequently present in solid tumors [7–10]. To better understand the consequences of chromosomal gains and losses resulting from the many structural aberrations detected with SKY and FISH, we further analyzed the genomic DNA with comparative genomic hybridization (CGH) [11]. A detailed molecular cytogenetic analysis of PB using CGH and SKY of the cell line reveals multiple chromosomal aberrations.

2. Materials and methods

2.1. Case report

The patient was a previously healthy 14-year-old black male who presented with a 2–3-month history of intermittent

* Corresponding author. Tel.: (301) 496-4256; fax: (301) 402-0575.
E-mail address: ct47@nih.gov (C.J. Thiele).

0165-4608/05/$ – see front matter © 2005 Elsevier Inc. All rights reserved.
doi:10.1016/j.cancergencyto.2004.05.017

abdominal pain, malaise, anorexia, and weight loss. Physical examination was notable for hepatomegaly to 15 cm below the right costal margin, and a 10-cm diameter left upper quadrant mass. Computed tomographic imaging revealed a left abdominal mass (12 cm × 10 cm × 15 cm diameter) with compression of the renal collecting system. There were metastatic lesions throughout the liver and peritoneal wall, as well as a 2.5-cm diameter pulmonary nodule. Diagnostic laboratory studies were notable for normal 24-hour urine catecholamine metabolites, β_2-microglobulin, and beta-human chorionic gonadotropin (B-HCG). The α-fetoprotein was mildly elevated, at 32 ng/mL (normal <9 ng/mL).

The initial course of therapy consisted of vincristine, doxorubicin with ICRF-187 (a cardioprotectant bispiperazinedione), and cyclophosphamide with mesna per National Cancer Institute protocol 86-C-169. His subsequent course was complicated by massive intraabdominal hemorrhage and irreversible multisystem organ failure. There was no demonstrable clinical or radiographic response by the tumor to the initial cycle of therapy. Electron micrographic studies of the biopsy subsequently became available, and revealed tumor cells oriented around a central lumen with surface microvilli and apical zymogen granules, consistent with a diagnosis of pancreatoblastoma. Given the new diagnostic information and the patient's apparently severe and irreversible organ dysfunction, 5-fluorouracil and leucovorin were administered with palliative intent. There was again no demonstrable response, and the patient died approximately 2 weeks later.

2.2. Histopathologic analysis

Immunohistochemical and electron microscopic analyses were done essentially as previously described [12].

2.3. Cell line and metaphase preparation

Tumor tissue from a needle biopsy was mechanically dissociated and cultured in RPMI 1640 supplemented with 10% fetal calf serum, glutamine, and antibiotics and the resulting cell line was named CMBS-PB. Metaphase chromosomes were harvested by means of mitotic shake-off following Colcemid treatment (10 μL/mL, 1 hour; Boehringer Mannheim [Roche Diagnostics], Mannheim, Germany). The cells were processed by means of standard cytogenetic methods using 0.075 mol/L KCl and fixative (methanol–acetic acid, 3:1) as described by Modi et al. [13]. SKY analysis was done at passages 2–5; DNA for CGH was obtained at passage 5. Karyotype analysis and ploidy of the primary tumor were not available.

2.4. Hybridization procedures and preparation of SKY and CGH probes

Prior to hybridization, the slides were stored at 37°C for 2 weeks, pretreated with pepsin to remove excess cytoplasm, and postfixed in formaldehyde (3% in 1× phosphate-buffered saline–50 mmol/L $MgCl_2$). The slides were denatured for 1–2 minutes in 70% formamide–2× SSC at 80°C and then hybridized with SKY probes. Subsequent CGH and FISH analysis involved the identical method for slide pretreatment. SKY probe was prepared from flow-sorted chromosomes, hybridized for 48 hours, and detected as described by Macville et al. [14]. Tumor DNA was extracted from cultured cells using the high-salt method(http://www.riedlab.nci.nih.gov/Protocols.asp) and then labeled with biotin via nick translation. For CGH, equal amounts (1 μg) of the biotin-labeled CMBS-PB DNA and digoxygenin-labeled normal human lymphocyte XY DNA were cohybridized on normal human XY lymphocyte metaphase chromosomes.

2.5. Image acquisition

Image acquisition of SKY-labeled metaphase cells was done via spectral cube and a charge-coupled device camera connected to a DMRXA microscope (Leica, Wetzlar, Germany) equipped with a custom-designed SKY-3 optical filter (Chroma Technology, Brattleboro, VT). SKY analysis was done using SkyView version 1.6.2 software (Applied Spectral Imaging, Migdal Ha'Emek, Israel). Image acquisition of FISH and CGH metaphase cells was done using Leica QFISH imaging software (Leica Imaging Systems, Cambridge, UK) using custom-designed filters (MF-102, TR2, TR3; Chroma Technology, Brattleboro, VT).

2.6. Cytogenetic analysis

SKY analysis of cell line CMBS-PB was done on 16 metaphase spreads. The cell line was further characterized using whole chromosome paints 1, 2, 3, 6, 7, 8, 11, 12, 13, 15, 16, 18, 19, 20, 21, 22, X, and Y (made using degenerate oligonucleotide primer–polymerase chain reaction), chromosome arm paint 1q (kindly provided by Mike Bittner, TGen, Phoenix, AZ), and a CMYC probe (Vysis, Downers Grove, IL) specific for the oncogene *MYC* (alias c-*MYC*). FISH analysis was done on 98 metaphase spreads. CGH analysis was done on 15 metaphase spreads, to yield a composite CGH profile.

3. Results

The light microscopic appearance of the abdominal tumor mass suggests an embryonal neoplasm composed of poorly differentiated, small round cells. Surgical biopsy of the mass revealed a poorly differentiated, small round blue cell tumor, with arrangement of some tumor cells around a lumen (Fig. 1A); elsewhere in the mass the cells formed whorls or exhibited ample pink cytoplasm, indicative of squamous differentiation (Fig. 1B). Electron microscopic evaluation revealed cells with overt acinar differentiation (as indicated by their orientation toward a central lumen with surface microvilli, junctional complexes, and zymogen granules), as well as primitive round cells. Detail of a junctional complex is shown

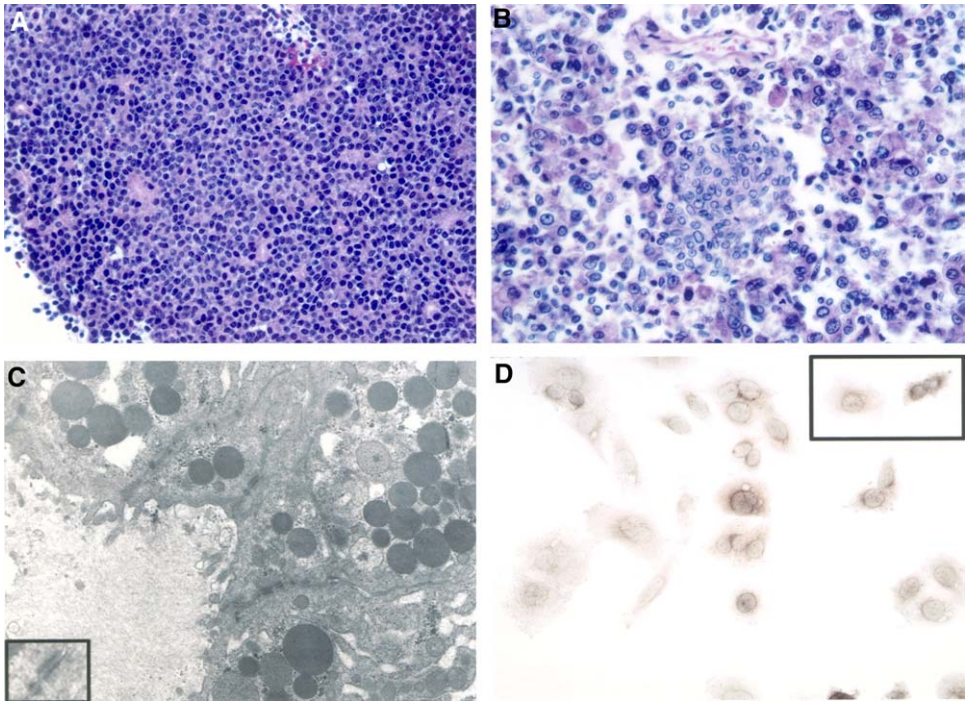

Fig. 1. (A,B) Light microscopic appearance of the abdominal tumor mass. The tumor is an embryonal neoplasm composed of poorly differentiated, small round cells. In many places, the tumor cells are arranged around a central lumen (A) and in others they form whorls or exhibit the ample pink cytoplasm indicative of squamous differentiation (B); hematoxylin–eosin staining; ×220. (C) Electron microscopic evaluation revealed cells with overt acinar differentiation—that is, cells oriented toward a central lumen with surface microvilli, junctional complexes, and zymogen granules—in addition to the primitive round cells; detail of a junctional complex is shown in the inset; uranyl acetate–lead citrate staining, ×13,780 (inset: ×46,500). (D) Immunocytochemical staining of cell line showed the tumor cells to be positive for α_1-antitrypsin (D) and keratin (inset); ×150.

in an inset in Fig. 1C. Immunocytochemical analysis revealed that the tumor cells were negative for neuron-specific enolase, chromogranin, Leu 7, desmin, muscle-specific actin, β_2-microglobulin, pancreatic polypeptide, amylase, and α-fetoprotein and positive for keratin (data not shown). The mixed histologic pattern, immunophenotypic staining, and ultrastructural appearance indicated that the tumor was PB.

A core needle biopsy was obtained and sequentially passed through increasingly fine-gauge needles to disperse clumps and the cell suspension was cultured in RPMI 1640 with 10% fetal calf serum; a continuous cell line CMBS-PB was established within 1 month (Figs. 1D and 2A). Immunocytochemical staining of the cell line was positive for α_1-antitrypsin (Fig. 1D) and keratin (Fig. 1D inset) and, like the tumor specimen, was negative for neuron-specific enolase, chromogranin, Leu 7, desmin, actin, β_2-microglobulin, pancreatic polypeptide, amylase, and α-fetoprotein (data not shown). In exponentially growing cells, cell cycle analysis revealed that, depending on the culture density, 40–45% of the cells were in the growth fraction (S+G2/M) (Fig. 2B). Some tumors of embryonal origin are sensitive to the growth-inhibiting and differentiating effects of retinoids [15]; however, even though the growth fraction of CMBS-PB decreased ~5% after a 6-day culture in 5 μmol/L all-trans retinoic acid, there was no dramatic morphologic change in the appearance of the cells (Fig. 2D) compared with control cells (Fig. 2C). There was no arrest of cells in G1 (data not shown).

3.1. G-banding analysis of CMBS-PB

The initial cytogenetic findings for this cell line were based on G-banded chromosomes (Fig. 3A). There were numerous structural aberrations that were difficult to interpret based solely on their G-banding patterns. G-banding showed 33 structurally aberrant chromosomes. CMBS-PB was hyperdiploid, with a chromosome number range of 48–60. With G-banding, eight aberrant chromosomes were described as marker chromosomes (M1–M7) (Fig. 3A).

3.2. SKY analysis

With the aid of SKY and FISH techniques, we could better characterize the complex aberrations present in this cell line. SKY analysis redefined 31 of 33 of the original aberrant chromosomes (Fig. 3B) seen with G-banding (Fig. 3A).

The composite karyotype is 48~60,+X[12],der(X)del(X)(p11.1)del(X)(q22)[12],+der(X)t(X;8)(q28;q23)t(8;21)(q24.3;q?)(CMYC+)t(8;21)(q24.3;q?)(CMYC+)t(8;21)(q?;q?)(CMYC−)[11],dic(X;19)(?::Xp22.1→Xq28::19p13.1→19q13.3::19q13.1→19qter)[8],−Y[16],trc(1;1;1)(qter;qter→p11;p11)del(1)(q11)[16],der(1)(7?::20?→20?::

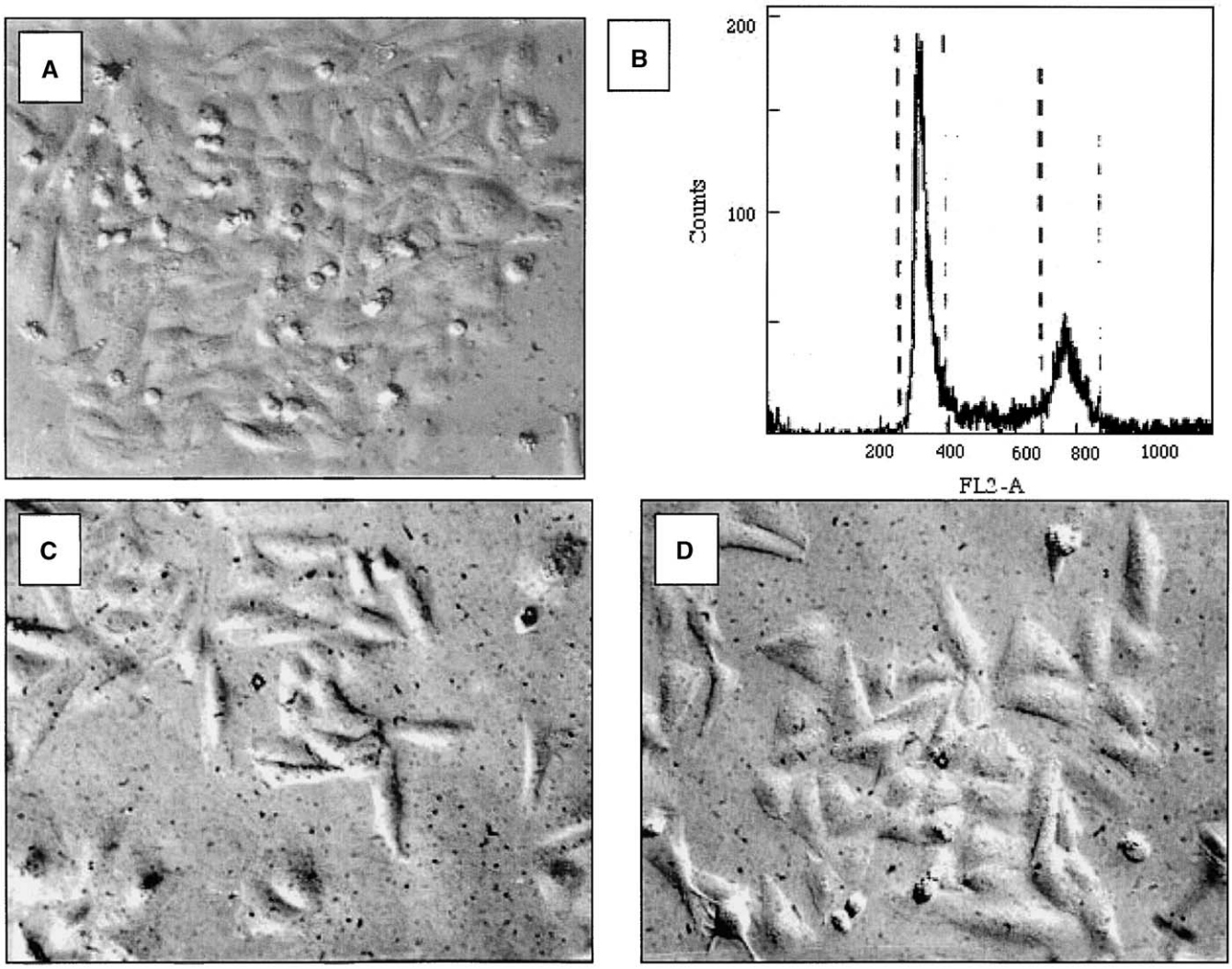

Fig. 2. (A) Light microscopic appearance of CMBS-PB grown in vitro. (B) DNA histogram of propidium iodine–stained CMBS-PB cells. (C,D) CMBS-PB cells cultured for 6 days in the presence of 5 μmol/L all-trans retinoic acid (D) or control solvent (C) and showed no signs of morphologic changes or changes in cell number.

8q24.3::15?::22?::1p32→1q25::13q14→13qter)(CMYC+)[15], +der(1)del(1)(p32)t(1;13)(q11;q?)del(13)(q?)[11], +der(1)del(1)(p13→q24)t(1;12)(q24;?)t(12;3)(?;?)t(3;1)(?;?)t(1;3)(?;?)t(3;6)(?;?)[10], del(2)(p23)[13], der(2)t(1;2)(p12;q11.2)t(1;2)(p?;?)[16], +der(2)del(p23)t(2;6)(q21;p15)[10], +der(2)del(2)(q23)t(1;6)(p?;?)t(2;6)(p13;?)[5], −3,der(3)(3pter→3q22::q13.1→qter)[15], +4[?],der(4)del(4)(q21)t(4;20)(q21;?)t(20;7)(?;?)[8],der(4)t(4;10)(q21;?)[6],4ace[7],der(6)t(2;6)(q12;p12)t(1;6)(p22;q21)[15],der(6)t(4;6)(q31.1;p21.3)[12], +del(6)(p11.2)[10], +der(6)t(1;6)(q32;q23)[9], +der(6)del(6)(p11.2)t(6;17)(q13;q21)t(8;17)(q13;q23)(CMYC+)[6],6ace[6],der(7)t(7;12)(p22;?)[5],der(7)t(7;20)(p22;p11.2)[14], del(8)(p12)[3], +der(8)t(8;12)(q24.1;?)[4], del(9)(p13)[8], +der(9)del(9)(p23)del(9)(q34.1)[8], +der(9)t(9;19)(q34.3;q13.1)[5], +del(10)(q11.2)[5],der(10)t(5;10)(?;p13)[12],der(11)t(4;11)(q27;p15)[12], der(12)t(3;12)(q22;q24.3)[10],der(12)t(12;17)(p11.2;q21)[12], +13,der(13)del(13)(q13)t(1;13)(p?;q13)t(1;13)(?;?)[13], +del(13)(q22q32)[2], +ins(13;1)(q13;q12q32)[1], +14[9],der(14)del(X)del(13)(q12)t(13;14)(p11.2;q34)[12],der(14)del(13)(q12)t(13;14)(p11.2;q34)[13],del(15)(q21q22)[12], +16,del(16)(p?)[8],der(16)t(12;16)(?;q22)[10], +der(16)t(16;17)(q22;q21)[9], +19[11], der(19)t(3;19)(q21;q13.3)[13],der(20)del(20)(p11.2)t(7;20)(q22;q13.2)[9],der(20)del(20)(p11.2)t(6;20)(?;q13.2)[10], +der(20)t(6;20)(q13.2;?)[9],der(21)del(21)(q22)t(8;21)(?;p11.2)[7], +der(21)t(8;21)(?;p11.2)[4], +22[13],del(22)(q13.1)[9],der(22)t(9;22)(?;?)[8], +der(22)t(5;22)(p13;p11.2)[6][cp16]. A graphic display of the composite karyotype (SKYgram) for CMBS-PB, with complete clinical and cytogenetic analysis details, is available at http://www.ncbi.nlm.nih.gov/sky/skyweb.cgi (L. Stapleton, submitter).

In 75% of the metaphase spreads analyzed, at least one normal copy of chromosomes 4, 5, 7, 9, 10, 11, 15, 16, 17, 18, 19, 21, and 22 was observed. Recurrent structural aberrations (primarily 54 unbalanced translocations and

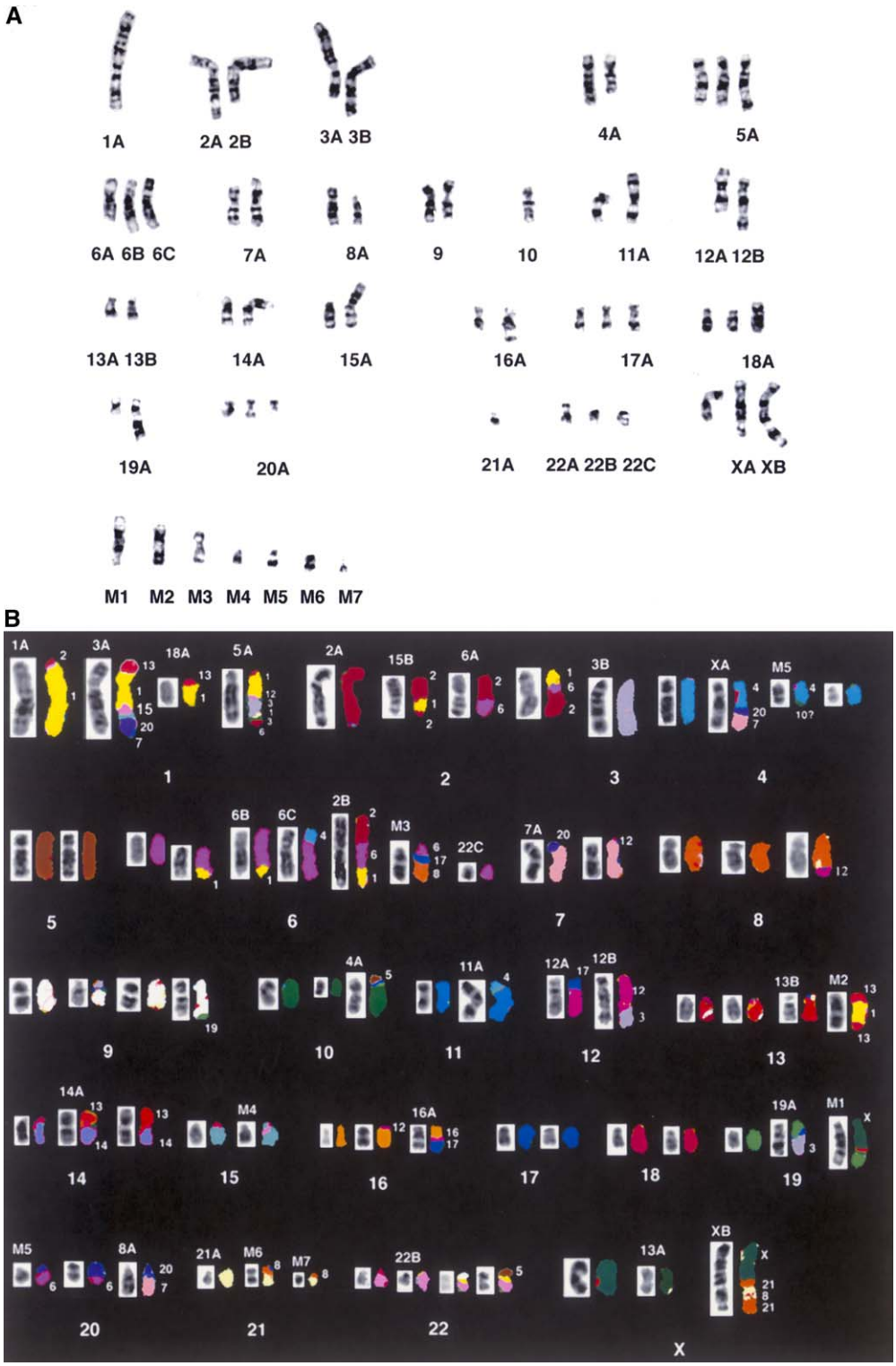

Fig. 3. (A) Original representative karyotype of CMBS-PB, passage 1, based on G-banding of chromosomes. (B) Composite karyotype of CMBS-PB, passages 2–5, based on SKY and FISH analysis. The designation of the aberrant chromosomes is the same in (A), for comparison purposes.

insertions) found with SKY occurred most often with chromosomes 1, 2, 3, 6, 7, 8, 12, 13, 14, 16, 19, 20, 21, 22, and X. No recurrent numerical aberrations were present (which is typical for many solid tumors), with the exception of clonal loss of the Y chromosome. In cell line CMBS-PB, the SKY analysis had limitations with respect to identifying translocations of highly rearranged chromosomes. For SkyView 1.6.2 to get concise classification, at least one normal copy of each chromosome needs to be present. SKY can detect segments as small as 1–2 kb; anything smaller can be

visualized more clearly with FISH. CMBS-PB does not have a complete set of normal chromosomes and in some cases multiple copies of single genes (e.g., *MYC*) were translocated to multiple chromosomes. FISH was done to confirm the SKY data.

3.3. CGH analysis

CGH analysis, which gives an overview of the whole genome, can explain what regions are gained or lost, but it does not clarify the manner in which they are rearranged. There were few whole chromosome arm amplifications; however, many segmental insertions and unbalanced translocations were present.

CGH (Fig. 4) revealed high regions of amplification of 1p→1q4, 6p, 7q21→7qter, 8q23→8qter, 17q22→17qter, 21q21→21qter, and whole chromosome X, and increased copy number of 2p22→2q11.2, 2q34→2qter, 3pter→3p21, 3q21→3qter, 4p15.3→4p11, 4q28→4qter, 6q, 9q21→9qter, 13, and 14q11.2→14q22, 20. CGH detected regions of loss on 1q43→1qter, 3p14→3p11, 8pter→8q13, 11q24→11ter, and Y. FISH, SKY, and CGH all confirmed the loss of the Y. It was important to further explore this cell line with FISH and SKY to better define the breakpoints of structural aberrations that were present.

SKY revealed 10 derivative chromosomes containing portions of chromosome 1 material; these data correlate with the CGH analysis showing regions of high amplification for chromosome 1. CGH showed a loss of 1q43→1qter, which was not apparent in the aberrations seen with SKY. For certain small pieces of chromosomes, SKY was unable to provide information regarding the origin, because the banding pattern was not informative. An example is the derivative chromosome 5A (Fig. 3B), which was found in 63% of SKY metaphases and 86% of FISH metaphases. FISH was done in this case to verify that the small inserted segments did indeed belong to chromosomes 3, 12, and 6, respectively. SKY was also able to identify five aberrant chromosomes that contained portions of chromosome 2. CGH results showed regions of gain at 2p22→2p10 and 2q32→2qter, which were likely involved in the translocations, as confirmed with FISH analysis using chromosome arm paints.

CGH showed an increased copy number in regions 3pter→3p14 and 3q22→3qter and a loss of 3p14→3q12. SKY analysis did not detect many structural aberrations involving chromosome 3 (Fig. 3B, chromosomes 3B and 19A). Because there were no normal copies of chromosome 3 present to aid the software in classification, FISH analysis was done and consequently we found two additional aberrant chromosomes containing chromosome 3 segments.

SKY identified a normal copy of chromosome 8 in 38% of metaphases and three aberrant marker chromosomes (Fig. 5A) present in more than 80% of metaphases. FISH was done to confirm the SKY data and four additional derivative chromosomes were found to contain small segments of 8 (Fig. 5A; M6, M7, XB, and 3A). The CGH data (Fig. 5B) showed a loss of 8p→8q13 and a gain of 8q23→8qter. SKY did not, however, discern what parts of chromosome 8 were

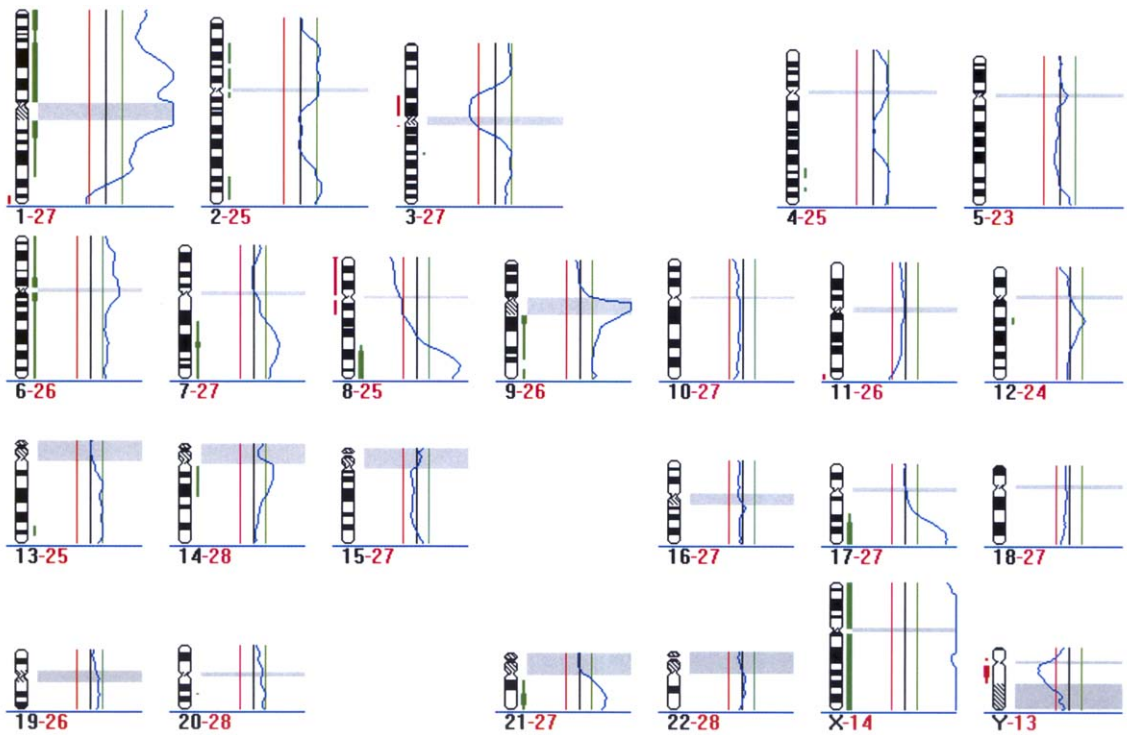

Fig. 4. CGH composite profile of CMBS-PB, passage 5, as generated from the 15 metaphases analyzed. Regions of loss are indicated with a red line to the left of the ideogram; regions of gain, a green line to the right. Centromeric regions, indicated by a gray bar, were disregarded throughout the analysis.

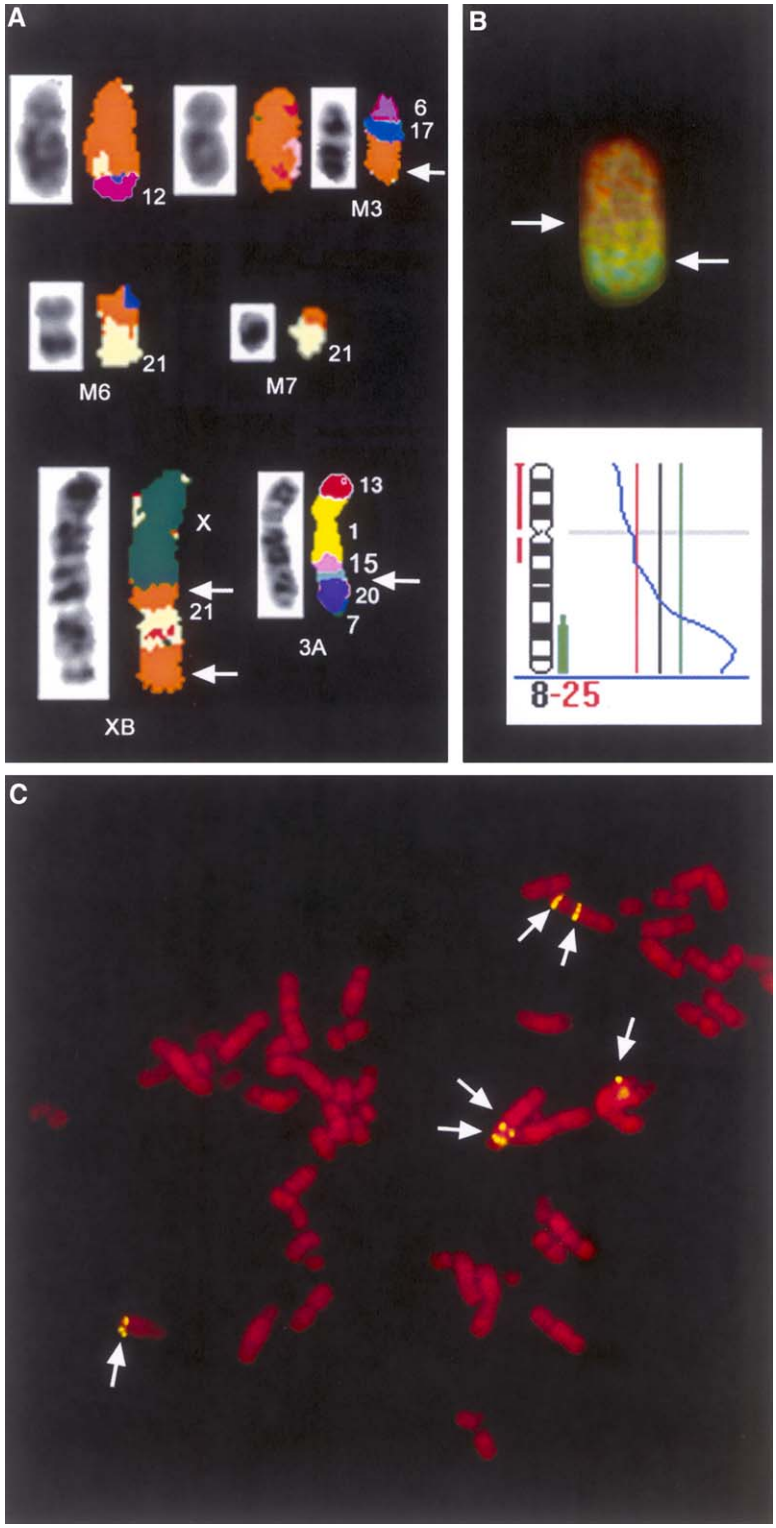

Fig. 5. (A) The seven aberrant chromosomes involving chromosome 8 aberrations as defined in the karyotype. Each chromosome is represented here with the inverted 4′,6-diamidino-2-phenylindole (DAPI) image alongside the SKY pseudocolor image as generated by SkyView 1.6.2 software. Arrows indicate presence of the *MYC* gene. (B) CGH data show regions of gain (green; arrow) and loss (red; arrow) along chromosome 8. This information is quantified and represented in the profile; regions of loss are indicated by a red line and regions of gain by a green line alongside the ideogram. (C) The CMYC probe (shown in yellow) was hybridized to metaphase slides of CMBS-PB to ascertain copy number. In this case, there were six copies (arrows) present in one metaphase.

involved in the chromosomal rearrangements. FISH using the probe for *MYC* (found at 8q24. 13) found multiple copies of this oncogene present in CMBS-PB (range 4–7 per cell) (Fig. 5C). Note that not all chromosome 8 aberrations contained a copy of *MYC*.

CGH showed a high region of amplification 17q22→17qter. SKY analysis revealed a normal complement of chromosome 17 plus three markers containing a piece of chromosome 17, probably consisting of the amplified region. Another example of a correlation between SKY and CGH results involves the X chromosome. CGH showed high amplification of the whole chromosome. SKY showed that there was one normal copy of the chromosome X present in 75% of metaphases. SKY identified four aberrations with chromosome X material (14A, 13A, XB, and M1) occurring in more than 70% of metaphases with either an insertion or translocation of X chromosome material (supported by FISH; data not shown).

4. Discussion

Although exceedingly rare, pancreatoblastoma (PB) is the most common of the pancreatic tumors in the pediatric population. Patients with pancreatoblastoma typically have a good prognosis; however, the patient from whom the CMBS-PB cell line was derived had no response to multimodal chemotherapy, progressed rapidly, and died. To our knowledge, this is the first description of a PB cell line, and this has enabled a comprehensive cytogenetic picture to be constructed. There are sporadic reports of cytogenetic analyses for PB, but no consistent chromosomal alterations have been identified. The initial chromosomal banding analysis of the CMBS-PB cell line in 1995 revealed 33 aberrant chromosomes; these were difficult to resolve, given the complexity of the rearranged chromosomes. We have now used SKY, FISH, and CGH analysis to delineate the complexity of the multiple alterations present in this cell line.

Abraham et al. [6] reported allelic loss on chromosome 11p in four of five informative cases out of seven pediatric PBs evaluated. These regions mapped to near the WT-2 locus on 11p15.5. In another case report, Kerr et al. [16] reported a karyotypically normal PB tumor with 11p LOH from the WT to the TH-IGF1-H19 loci, although no mutations in *WT1* were detected. The CMBS-PB cell line has a der(11)t(4;11)q27;p15) consistent with an alteration in this region, but CGH analysis did not reveal any significant gains or losses in 11p. Mutations in β-catenin have also been found in four of seven pediatric PB tumors [6]. We did not address the issue of potential gene mutations in our analysis, but plan future studies to assess whether the β-catenin pathway is altered in this cell line. Haag et al. [17] reported a case of a 3.5-year-old patient whose tumor responded to chemotherapy and was completely resected and in which a short-term culture showed an abnormal clone with a hyperdiploid karyotype showing trisomy for chromosomes 7, 8, and 10, tetrasomy for chromosome 12, and a der(15)t(1:15)(q21;p11.2). Gains of chromosomes 7, 8, and 12 have been reported in adult pancreatic carcinoma [17].

In pancreatic carcinoma, complex karyotypes and multiple marker chromosomes have presented challenges in establishing a cytogenetic picture [18]. The CMBS-PB cell line contains multiple marker chromosomes and alterations of virtually every chromosome. CGH revealed numerical gains for chromosomes 1, 6, and X, gains for chromosome arms 2q, 7q, 8q, 17q, and 21q, and smaller gains in specific areas of chromosomes 2, 3, 4, 12, 14 and 19. CGH revealed loss in chromosome arms 8p and 11q and in the Y chromosome. The 8q gain in the CMBS-PB cell line is similar to a region that is gained in adult pancreatic carcinomas and that includes the *MYC* gene [18].

Complete excision results in cure in most cases of pediatric pancreatoblastoma; however, the patient from whom the cell line CMBS-PB was derived presented with metastatic disease and failed to respond to therapy. Whether the complexity of the chromosomal alterations contributed to the particularly fulminating progression of this tumor cannot be determined; however, the karyotypic analysis of this cell line contributes to the emerging picture of the complexity of genetic aberrations leading to pancreatic tumorigenesis. Analysis of additional cases will be needed to define recurrent events in pancreatic tumorigenesis. Finally, the isolation and analysis of this cell line may enable the development of in vitro and in vivo assays to assess potential therapies for this rare tumor.

Acknowledgments

We would like to thank Dr. William Nash for providing the initial G-banded karyotype as seen in Fig. 3A and Turid Knutsen and Dr. Jackie Whang-Peng for initial cytogenetic advice on this tumor.

References

[1] Greenlee RT, Murray T, Bolden S, Wingo PA. Cancer Statistics, 2000. [Available at http://caonline.amcancersoc.org/cgi/reprint/50/1/7.] CA Cancer J Clin 2000;50:7–33.

[2] Pratt CB, Pappo AS. Management of infrequent cancers of childhood. In: Pizzo PA, Poplack DG, editors. Principles and practice of pediatric oncology. 4th edition. Philadelphia: Lippincott Williams & Wilkins, 2002, pp. 1157–8.

[3] Riesener K, Kasperk R, Fuzesi L, Schumpelick V. Pancreatoblastoma: ultrastructural and image DNA cytometric analysis. Dig Surg 2001; 18:78–82.

[4] Wiley J, Posekany K, Riley R, Holbrook T, Silverman J, Joshi V, Bowyer S. Cytogenetic and flow cytometric analysis of a pancreatoblastoma. Cancer Genet Cytogenet 1995;79:115–8.

[5] Nagashima Y, Misugi K, Tanaka Y, Ijiri R, Nishihira H, Nishi T, Kigasawa H, Kato K. Pancreatoblastoma: a second report on cytogenetic findings. Cancer Genet Cytogenet 1999;109:178–9.

[6] Abraham SC, Wu T-T, Klimstra DS, Finn LS, Lee J-H, Yeo CJ, Cameron JL, Hruban RH. Distinctive molecular genetic alterations

in sporadic and familial adenomatous polyposis-associated pancreatoblastoma: frequent alterations in the APC/β-catenin pathway and chromosome 11p. Am J Pathol 2001;159:1619–27.

[7] Knutsen T, Ried T. SKY: a comprehensive diagnostic and research tool: a review of the first 300 published cases. J Assoc Genet Technol 2000;26:3–15.

[8] Schröck E, Padilla-Nash H. Spectral karyotyping and multicolor fluorescence in situ hybridization reveal new tumor-specific chromosomal aberrations. Semin Hematol 2000;37:334–47.

[9] Phillips JL, Ghadimi BM, Wangsa D, Padillla-Nash H, Worrell R, Hewitt S, Walther M, Linehan WM, Klausner RD, Ried T. Molecular cytogenetic characterization of early and late renal cell carcinomas in von Hippel–Lindau disease. Genes Chromosomes Cancer 2001; 31:1–9.

[10] Schröck E, du Manoir S, Veldman T, Schoell B, Wienberg J, Ferguson-Smith MA, Ning Y, Ledbetter DH, Bar-Am I, Soenksen D, Garini Y, Ried T. Multicolor spectral karyotyping of human chromosomes. Science 1996;273:494–7.

[11] Kallioniemi OP, Kallioniemi A, Sudar D, Rutovitz D, Gray JW, Waldman F, Pinkel D. Comparative genomic hybridization: a rapid new method for detecting and mapping DNA amplification in tumors. Semin Cancer Biol 1993;4:41–6.

[12] Parham DM, Hijazi Y, Steinberg SM, Meyer WH, Horowitz M, Tzen CY, Wexler LH, Tsokos M. Neuroectodermal differentiation in Ewing's sarcoma family of tumors does not predict tumor behavior. Hum Pathol 1999;30:911–8.

[13] Modi WS, Nash WG, Ferrari AC, O'Brien SJ. Cytogenetic methodologies for gene mapping and comparative analysis in mammalian cell culture systems. Gene Anal Tech 1987;4:75–85.

[14] Macville M, Veldman T, Padilla-Nash H, Wangsa D, O'Brien P, Schröck E, Ried T. Spectral karyotyping, a 24-colour FISH technique for the identification of chromosomal rearrangements. Histochem Cell Biol 1997;108:299–305.

[15] Gaetano C, Matsumoto K, Thiele CJ. In vitro activation of distinct molecular and cellular phenotypes after induction of differentiation in a human neuroblastoma cell line. Cancer Res 1992;52:4402–7.

[16] Kerr NJ, Chun Y-H, Yun K, Heathcott RW, Reeve AE, Sullivan MJ. Pancreatoblastoma is associated with chromosome 11p loss of heterozygosity and IGF2 overexpression. Med Pediatr Oncol 2002;39:52–4.

[17] Haag MM, Sutcliffe MJ, Dumont DP, McFarland JA, Favara BE, Chamizo W. Cytogenetic findings in rare pediatric tumors: report of a case of interdigitating reticulum cell sarcoma and a case of pancreatoblastoma. Cancer Genet Cytogenet 1995;84:158.

[18] Ghadimi BM, Schrock E, Walker RL, Wangsa D, Jauho A, Meltzer PS, Ried T. Specific chromosomal aberrations and amplification of the AIB1 nuclear receptor coactivator gene in pancreatic carcinomas. Am J Pathol 1999;154:525–36.